

The role of reactive oxygen species in the virulence of wheat leaf rust fungus *Puccinia triticina*

Xiben Wang ^{1*}, Mingzhe Z. Che,^{1,2} Hala B. Khalil,^{3,4} Brent D. McCallum,¹ Guus Bakkeren,³ Christof Rampitsch¹ and Barry J. Saville⁵

¹Morden Research & Development Centre, Agriculture and Agri-Food Canada, 101 Route 100, Morden, Manitoba, R6M 1Y5, Canada.

²Department of Plant Pathology, College of Agriculture and Biotechnology, China Agricultural University, No. 2 Yuan Ming Yuan West Road, People's Republic of China.

³Summerland Research & Development Centre, Agriculture and Agri-Food Canada, Summerland, British Columbia, V0H 1Z0, Canada.

⁴Department of Genetics, Faculty of Agriculture, Ain Shams University, 68 Hadayek Shoubra, Postal code, Cairo, 11241, Egypt.

⁵Forensic Science Program Trent University, Peterborough, Ontario, K9J 7B8, Canada.

Summary

Reactive oxygen species (ROS) play an important role during host–pathogen interactions and are often an indication of induced host defence responses. In this study, we demonstrate for the first time that *Puccinia triticina* (*Pt*) generates ROS, including superoxide, H₂O₂ and hydroxyl radicals, during wheat infection. Through pharmacological inhibition, we found that ROS are critical for both *Pt* urediniospore germination and pathogenic development on wheat. A comparative RNA-Seq analysis of different stages of *Pt* infection process revealed 291 putative *Pt* genes associated with the oxidation–reduction process. Thirty-seven of these genes encode known proteins. The expressions of five *Pt* genes, including *PtNoxA*, *PtNoxB*, *PtNoxR*, *PtCat* and *PtSod*, were subsequently verified using RT-qPCR analysis. The results show that the expressions of *PtNoxA*, *PtNoxB*, *PtNoxR*, *PtCat* and *PtSod* are up-regulated during urediniospore germination. In comparison, the expressions of *PtNoxA*, *PtNoxB*, *PtNoxR* and *PtCat* are down-regulated during wheat infection

from 12 to 120 h after inoculation (HAI), whereas the expression of *PtSod* is up-regulated with a peak of expression at 120 HAI. We conclude that ROS are critical for the full virulence of *Pt* and a coordinate down-regulation of *PtNox* genes may be important for successful infection in wheat.

Introduction

The generation of reactive oxygen species (ROS) is a common mechanism found in both eukaryotic and prokaryotic organisms which leads to the formation of several reactive oxygen radicals, ranging from relatively unreactive superoxide (O₂^{•−}) and hydrogen peroxide (H₂O₂) to highly reactive oxygen species (hROS). The hROS may exist as free hydroxyl radicals (HO[•]), as bound ('crypto') radicals or as Fe(IV)-oxo (ferryl) species (Freinbichler *et al.*, 2011). These radicals play diverse roles in cell physiology and regulate cell immunity, proliferation, differentiation, signal transduction and ion transport (Aguirre *et al.*, 2005; Bashandy *et al.*, 2010; Dietz *et al.*, 2016; Marschall and Tudzynski, 2016).

During host–pathogen interactions, plant cells are capable of producing an 'oxidative burst' in response to the pathogen infection. The production of ROS is often one of the earliest manifestations of the host defence response (Wojtaszek, 1997; Dietz *et al.*, 2016; Sewelam *et al.*, 2016). These radicals can kill the pathogen directly, strengthen the plant cell wall through oxidative cross-linking of structural compounds or function in the programmed cell death (Torres *et al.*, 2006). In plants, NADPH oxidases (Nox) play an important role in the generation of ROS which are involved in a wide range of plant physiological and defence responses (Foreman *et al.*, 2003; Kwak *et al.*, 2003). Several studies have suggested that plant-derived ROS generated by membrane-bound Nox and apoplast-secreted peroxidase are involved in the host defence response to cereal rust fungi (Fofana *et al.*, 2007; Dmochowska-Boguta *et al.*, 2013).

In the filamentous fungi, the generation of ROS through Nox plays an important role in virulence and cellular differentiation. The production of ROS is critical for the differentiation of appressoria in *Magnaporthe grisea* (Egan *et al.*, 2007; Ryder *et al.*, 2013) and the strengthening of

Received 29 August, 2017; revised 4 May, 2020; accepted 5 May, 2020. *For correspondence. E-mail xiben.wang@canada.ca; Tel. 1-204-3120593; Fax 1-204-822-7507.

penetration pegs in *Verticillium dahliae* (Zhao *et al.*, 2016) and in *Alternaria alternata* (Hyon *et al.*, 2010). Studies have shown that free ROS radicals are associated with the spore germination in *M. grisea* (Egan *et al.*, 2007) and *Neurospora crassa* (Michan *et al.*, 2002). In the initial stage of colonization by arbuscular mycorrhizal (AM) fungi, a rapid ROS burst is often triggered in the host plant. AM symbiosis is capable of increasing activities of antioxidant enzymes and reinforces the antioxidant defence system of the host plant for the prevention of oxidative damage (Kapoor and Singh, 2017). The adaptation to oxidative stress in *G. margarita* differs depending on the presence/absence of endobacterium. *G. margarita* with its endobacterium produces more ROS and has a higher ROS-detoxifying capacity than a cured line that lacks the endobacterium (Venice *et al.*, 2017). The relevant information regarding the role of ROS in the pathogenesis of biotrophic fungi is sparse. In *Claviceps purpurea*, the production of ROS mediated by CpNox1 impacts cellular growth, vegetative differentiation and normal pathogenic development (Giesbert *et al.*, 2008). *Ustilago maydis* uses an H₂O₂ detoxification system to cope with early plant defence responses during its infection on maize (Molina and Kahmann, 2007). It has also been shown that nitric oxide (NO) and ROS coordinately act as signalling molecules in the pre-infection development of *Puccinia striiformis* f. sp. *tritici* (*Pst*) and the polarized growth of *Pst* germ tubes (Yin *et al.*, 2016).

Puccinia triticina Eriks (*Pt*) is an obligate parasitic fungus causing leaf rust disease on wheat (*Triticum aestivum*). The infection of *Pt* on wheat starts with the deposition of urediniospores on the leaf surface. Upon germination, germ tubes grow perpendicular to leaf veins until they encounter stomata. Once stomata are recognized, the penetration takes place through the formation of appressoria and substomatal vesicles. The initiation of the intercellular infection involves the formation of haustorial mother cells, haustoria as well as secondary infection hyphae (Leonard and Szabo, 2005).

Currently, the role of ROS in the virulence of *Pt* is unknown. Hence, we used a set of dyes to visualize ROS generated by *Pt* during infection. We present histological and cytochemical evidence showing that ROS, including O₂^{•-}, H₂O₂, and possibly HO[•], are produced by *Pt* during wheat infection. Through pharmacological inhibition, we demonstrate that a concerted production of these radicals is required for the full virulence of this pathogen. The availability of the *Pt* draft genome has opened up opportunities to investigate key *Pt* genes associated with the oxidation–reduction process. We conducted a time-course RNA-Seq analysis to identify *Pt* genes associated with this process. The expressions of five candidate *Pt* genes during urediniospore germination and *in planta* were subsequently verified using RT-qPCR.

Materials and methods

Fungal strain and plant growth condition

Pt race BBBB was increased from a single-pustule inoculation in the greenhouse, and virulence phenotype was verified on a differential set containing 16 Thatcher NILs as described by McCallum *et al.* (2013). Susceptible wheat cultivar Thatcher was grown in the greenhouse. Freshly collected *Pt* urediniospores were used in this study to ensure a high germination rate (>90%).

Chemicals and treatments

Diphenylene iodonium (DPI), salicylhydroxamic acid (SHAM), 2,2,6,6-tetramethylpiperidine-*N*-oxyl (TEMPO), mannitol and uric acid were purchased from Sigma (Oakville, ON, Canada). These chemicals were added to 2% water agar in the germination test or used as solutions as described below in detached leaf/whole plant assays.

MitoSOX Red (5 mM, Invitrogen, Canada) was used for the visualization of O₂^{•-}. This dye is live-cell permeable and emits red fluorescence when selectively oxidized by O₂^{•-} (Robinson *et al.*, 2006). Hydroxyphenyl fluorescein (HPF) was used to detect hROS. HPF reacts selectively with HO[•] and peroxyxynitrite (ONOO⁻), and it is inert against O₂, O₂^{•-}, H₂O₂ and NO (Setsukinai *et al.*, 2003). The general status of ROS in *Pt* infection-related structures was evaluated using 2',7'-dichlorodihydrofluorescein diacetate (H₂DCF-DA) reacting with several commonly produced ROS (Chernyak *et al.*, 2006). A working solution of 60 mM nitroblue tetrazolium (NBT) in 20 mM phosphate buffer (pH 6.1) was prepared for the detection of O₂^{•-}. A working solution of 0.7 mg 3,3'-diaminobenzidine (DAB)/ml in 60 mM Tris buffer (pH 8.0) was used to detect H₂O₂.

Microscopic analysis of *Pt* ROS production

Five micromole MitoSOX Red reagent in Hank's balanced salt solution (Life Technologies, Canada), 15 μM HPF in 0.1 M sodium phosphate buffer (pH 7.4) and 10 μM H₂DCF-DA in 0.1 M Tris–HCl (pH 7.4) were used in the fluorescent microscopy. A working solution of 0.7 mg DAB/ml in 60 mM Tris buffer (pH 8.0) was used to detect H₂O₂. Wheat leaves were cut into 1-cm long segments and incubated with 1.5 ml staining solution in 2 ml Eppendorf tubes for 1 h in dark at room temperature. The leaf segments were then transferred to a microscope slide and covered with a cover slide. The red fluorescence emitted from MitoSOX Red within *Pt* structures was examined using a Leica Cy3 fluorescence filter cube (excitation filter 545 nm). The signal emitted from HPF and H₂DCF was visualized with a Leica I3 fluorescence filter cube (excitation filter, 450–490 nm; dichromatic Mirror, 510 nm; and suppression filter, 515 nm). The presence of H₂O₂ and

$O_2^{\cdot-}$ through the staining of DAB and NBT was assessed under a Leica bright field microscope. Uvtex2B was used at 0.1% (w/v) in the staining solution as a counterstain to highlight *Pt* structures, using the method described by Wang *et al.* (2012)

Detection of ROS in *Pt* infection structures

Seven-day-old wheat plants at the two-leaf stage were spray inoculated with a *Pt* urediniospore-oil (Bayol, Imperial oil limited, Canada) suspension at a concentration of 1×10^6 urediniospores/ml. After inoculation, oil was evaporated for 1 h at room temperature. Plants were incubated in a moisture chamber at 18°C and 100% relative humidity overnight and then transferred to the greenhouse. For the detection of ROS in *Pt*-infected tissues, leaves were infiltrated with NBT, DAB and HPF as described above using a Hagborg device (Hagborg, 1970) and incubated at the room temperature for 3 h. Then, leaves were detached, and the presence of ROS intermediates was assessed under a Leica DMRB microscope.

Effects of antioxidants on germination and growth of *Pt*

Pt urediniospores were germinated on 2% water agar containing 100 μ M uric acid, 250 μ M DPI, 25 mM SHAM, 250 mM mannitol and 25 mM TEMPO (2,2,6,6-tetramethylpiperidinyloxy). Urediniospores germinated on 2% water agar were used as the blank control. DPI inhibits the production of $O_2^{\cdot-}$ mediated by flavoenzymes, particularly NADPH oxidase. SHAM is a potent class III peroxidase inhibitor, whereas TEMPO is routinely used as a superoxide dismutase mimic. Mannitol is a HO^{\cdot} scavenger. Uric acid is used as a scavenger for peroxyxynitrite. Germination rates were estimated at 24 h after urediniospores were dusted onto the agar and 20 different counts were conducted, each including 100–150 urediniospores. Wheat leaves were infiltrated with 100 μ M DPI and 10 mM SHAM using a Hagborg device 3 h before the inoculation with *Pt* race BBBB. Symptoms were rated 7 days after inoculation (DAI). Leaves infiltrated with double distilled water were used as blank control. For each treatment, 20 inoculated leaves were analysed using Assess 2.0 (American Phytopathological Society) for the percentage of leaf area covered by pustules.

Visualization of *Pt* infection hyphae and imaging analysis

Pt colonies in infected leaves were visualized with Uvitex2B using the method described by Wang *et al.* (2012). Images were captured using either a colour Leica DC295 camera or a black and white FX360 digital camera. The overlay of images was created using the Leica image overlay module (Leica).

RNA-Seq analysis

Total RNA was extracted from *Pt* urediniospores germinated over water for 24 h and from first leaves of wheat plants at 12, 24, 36 and 48 h after inoculation (HAI), as well as 5 and 7 DAI using TRIzol® (Sigma-Aldrich, Oakville, Canada), according to the procedure described by the manufacturer. All libraries were sequenced using Illumina technology at the Michael Smith Genome Sciences Center in Vancouver, BC, Canada (Supplemental Table S1). Quality control analysis of Illumina reads was carried out by deleting contiguous nucleotides with a Phred score less than 20 from the ends of the reads and masking internal nucleotides with a Phred score less than 20 with N's using the FASTQ quality trimmer and FASTQ masker tools from the FASTX package tool, (http://hannonlab.cshl.edu/fastx_toolkit/). High-quality reads of each library were aligned to the *Pt* race BBBB version 2 reference genome (NCBI assembly ADAS00000000, BioProject PRJNA36323) (Cuomo *et al.*, 2017) using STAR aligner (Dobin *et al.*, 2013) with default parameters. The *Pt* transcript abundance was reported as the normalized fragment per kilobase per million (FPKM) value, which was normalized using Cuff-link (Trapnell *et al.*, 2010) based on the read depth of each library and the length of each *Pt* reference gene.

Gene ontologies

Gene ontology (GO) enrichment annotation of *Pt* genes was characterized via a database at FungiFun (<https://elbe.hki-jena.de/fungifun/fungifun.php>, release updated at 20 November, 2014). *Pt* genes were defined by the GO term and grouped in different categories based on their GO definition. Genes involved in the oxidation–reduction process were analysed for their relative transcript abundance based on the FPKM values.

Phylogeny and sequence analysis

Protein sequences of Nox from selected fungal species were retrieved from UniprotKB database (<http://www.uniprot.org/>) and aligned using the MAFFT program with default parameters (Katoh and Standley, 2013). The phylogenetic trees were constructed with MEGA5 using the neighbour-joining method (Tamura *et al.*, 2011) and rooted with *Homo sapiens* Nox1 (Q9Y5S8) for PtNoxA and PtNoxB and with *Dictyostelium discoideum* NoxR (Q87T7) for PtNoxR. The number at the node indicates the percentage of 1000 bootstrap replicates that support each labelled interior branch. The proteins sequences of vertebrate p67^{phox} and fungal NoxR were aligned using the ClustalX program, and the conserved motifs were

searched over the server PROSITE (<https://prosite.expasy.org/>).

RNA extraction, cDNA synthesis and quantitative real-time PCR

Total RNA was extracted from *Pt* urediniospores germinated on water and infected wheat leaves using a QIAGEN RNA mini kit following the manufacturer's instructions (Qiagen, Mississauga, Canada). RNA samples were treated with QIAGEN RNase-Free DNase (Qiagen, Mississauga, Canada). The quality and quantity of RNA were determined using ethidium bromide-stained agarose gels and a NanoDrop-1000 spectrophotometer (NanoDrop Technologies, Toronto, Canada). First-strand cDNA was synthesized from 1 µg of total RNA in a final volume of 20 µl using iScript™ reverse transcription supermix (Biorad, Mississauga, Canada), according to the manufacturer's instructions.

The qPCR was performed on a CFX96™ machine (Bio-Rad, Mississauga, Canada). Specific primers for each gene were designed using PRIMER 3.0 and listed in Supplemental Table S2. The qPCR was conducted in a 12.5 µl volume using SsoFast evaGreen supermix (Bio-Rad, Mississauga, Canada). Thermal cycling parameters were: 98°C for 2 min, followed by 39 cycles of 95°C for 10s and 60°C for 30s. All products were subjected to melting curve analysis between 65°C and 95°C, to determine the specificity of the PCR reaction. There were three biological repeats for each time point, and three technical replicates were performed on each sample. RT-qPCR data were normalized to *Pt* succinate dehydrogenase transcripts as described by Panwar *et al.* (2013). The relative transcript level was calculated using the $2^{-\Delta\Delta C_t}$ method as described by Livak and Schmittgen (2001).

Results

The production of ROS by *Pt* during wheat infection

Pt race BBBB is fully virulent on the wheat cultivar Thatcher. MitoSOX Red, DAB, H₂DCFDA and HPF were used to detect O₂^{•-}, H₂O₂, ROS and hROS respectively (Fig. 1). At 3 HAI, both O₂^{•-} (MitoSOX red, Fig. 1b) and H₂O₂ (DAB, Fig. 1g) were detected in *Pt* urediniospores and emerging germ tubes. At 6 HAI, germ tubes start to produce appressoria over wheat stomata. At this stage, these two radicals were mostly detected in appressoria (Fig. 1c and h). This is expected because the cytoplasm normally migrates from the germ tubes into the developing appressoria. Subsequently, O₂^{•-} and H₂O₂ were detected in substomatal vesicles and primary infection hyphae at 12 HAI but not in wheat stomatal guard cells associated with these *Pt* structures (Fig. 1d and i). Post

48 HAI, most *Pt* structures remaining on the leaf surface no longer contained any of these two radicals (Fig. 1e and j).

ROS produced in *Pt* infection structures were visualized using H₂DCFDA reacting to a wide range of ROS. H₂DCFDA is primarily used to detect O₂^{•-} and H₂O₂ but also reacts to hROS. During the early infection stage (0–6 HAI, Fig. 1k–m), the localization of ROS reacting with H₂DCFDA was very similar to those seen with MitoSOX Red (O₂^{•-}) and DAB (H₂O₂). However, the fluorescent signal emitted from oxidized DCF was detected in stomatal guard cells in contact with *Pt* appressoria at 12 HAI (Fig. 1n). The difference between the pattern of ROS distribution revealed using MitoSOX Red/DAB and that of H₂DCFDA suggests that radicals other than O₂^{•-} and H₂O₂ are produced during *Pt* penetration process.

We subsequently investigated the production of hROS during *Pt* infection using HPF, a fluorescent dye reacting selectively with two hROS radicals including hydroxyl radicals, and peroxyxynitrite anions. The localization of hROS revealed using HPF was similar to that seen with H₂DCFDA. The generation of hROS was first detected within 3 HAI in germinating urediniospores and emerging germ tubes (Fig. 1q) and then found in appressoria at 6 HAI (Fig. 1r) and later in guard cells of wheat stomata in contact with *Pt* appressoria at 12 HAI (Fig. 1s). At 48 HAI, hROS were no longer detected in *Pt* structures remaining on the leaf surface (Fig. 1t).

ROS in *Pt* structures produced during wheat infection were also investigated through the infiltration of infected leaves with NBT, DAB and HPF, reacting to O₂^{•-}, H₂O₂ and hROS respectively (Fig. 2). At 3 DAI, all radicals were abundantly produced in *Pt* intercellular infection hyphae and haustoria (Fig. 2b, c, e, f, h and i). These radicals were not detected at all in mesophyll cells of non-inoculated wheat leaves (Fig. 2a, d and g) and mesophyll cells surrounding *Pt* infection sites in inoculated leaves.

Antioxidants and ROS scavengers reduce *Pt* germination and virulence

A set of pharmacological inhibitors was used to evaluate the role of ROS in *Pt* urediniospore germination and virulence on wheat. DPI, SHAM, mannitol, and TEMPO all inhibited the germination of urediniospores whereas uric acid had no inhibitory effect (Fig. 3a). At 7 DAI, there were fewer pustules on the leaf surface in wheat leaves infiltrated with DPI or SHAM (Fig. 3b), and the percentage of leaf area covered by pustules was reduced by more than 75% (Fig. 3c), compared to the control. In addition, *Pt* colonies in wheat leaves infiltrated with DPI or SHAM were smaller compared to those produced in the control at 2 and 5 DAI (Fig. 3d).

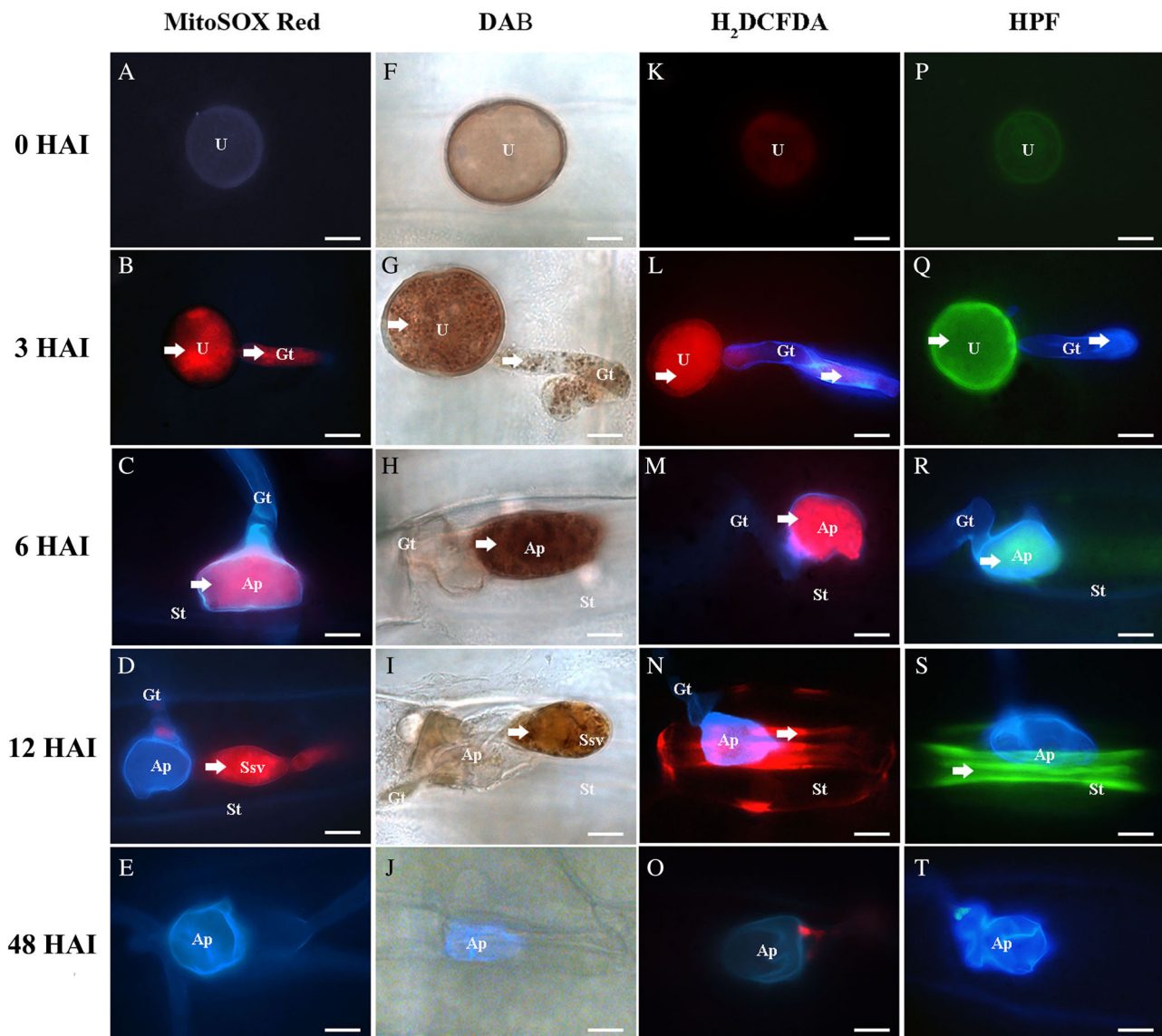


Fig 1. The generation of ROS during the infection of *Pt* on wheat. Superoxide, hydrogen peroxide, ROS and hROS produced by *Pt* were detected using MitoSOX Red (A–E), DAB (F–J), H₂DCFDA (K–O) and HPF (P–T) respectively. Leaves were collected at 3, 6, 12 and 48 HAI. U, urediniopores; Gt, germ tube; Ap, appressorium; Ssv, substomatal vesicle, St, wheat stomata. The arrows indicated the generation of ROS in *Pt* infection-related structures and scale bars represented 10 μ m. [Color figure can be viewed at wileyonlinelibrary.com]

RNA-seq analysis of *Pt* genes related to the oxidation–reduction

To identify *Pt* genes associated with the oxidation–reduction and to profile their expression during wheat infection, a detailed RNA-Seq experiment was carried out (Supplemental Table S1). After quality check and data cleaning, 890.36 million high-quality reads were obtained with 138.33 million reads aligned to *Pt* reference genome sequences. The percentage of reads mapped to *Pt* reference genome was the lowest at 12 HAI (5.63%) and the highest at 5DAI (59.8%). A total of 3491 *Pt* unique transcripts were annotated with at least one GO term. These

transcripts were categorized into 18 functional groups using Blast2GO. The group of the ‘metabolic process’ consisted of the largest portion of *Pt* transcripts followed by the ‘nucleotide-binding’ and the ‘oxidation–reduction’. Of note, 291 *Pt* transcripts were related to the oxidation–reduction process (Supplemental Fig. S1a), and 37 of them encoded known proteins (Supplemental Fig. S1b and Table S3). PTTG_29051 (a putative *PtNoxA*), PTTG_08931 (a putative *PtNoxB*) and PTTG_05336 (a putative *PtNoxR*) showed sequence similarities to genes encoding a NoxA, a NoxB and a regulatory NoxR respectively (Fig. 4). Two *Pt* genes, *PtCat* (PTTG_06754)

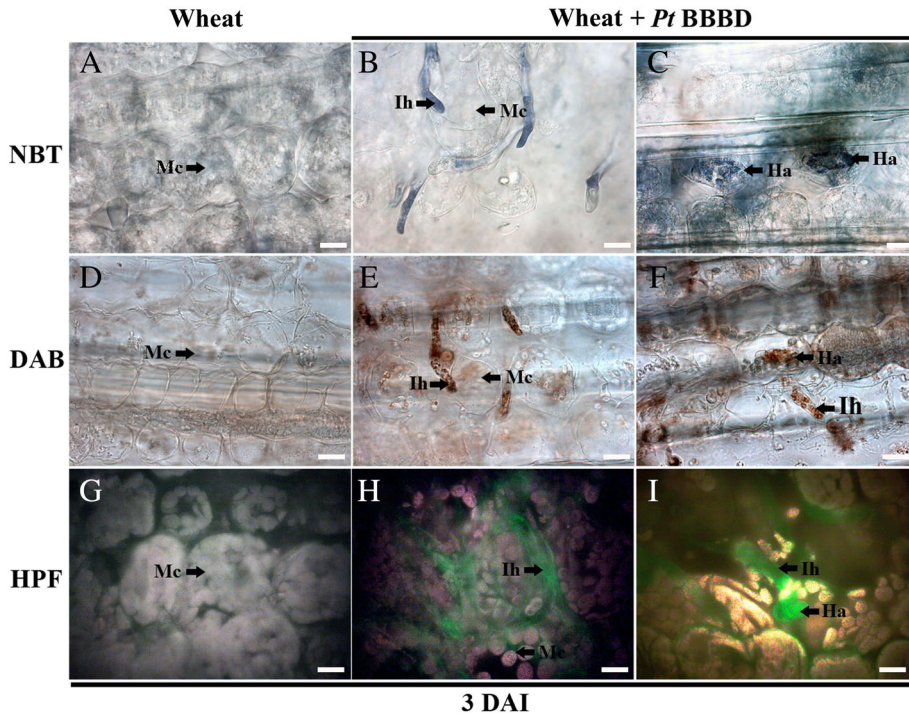


Fig 2. The generation of ROS in *Pt* infection-related structures. Wheat leaves inoculated with *Pt* race BBBD were collected 3 DAI and then infiltrated with aqueous solutions of NBT (A–C), DAB (D–F) and HPF (G–I). Ih, infection hyphae; Mc, mesophyll cell; Ha, haustorium. The arrows indicated the generation of ROS in *Pt* infection-related structures. Scale bars represented 10 μm . [Color figure can be viewed at wileyonlinelibrary.com]

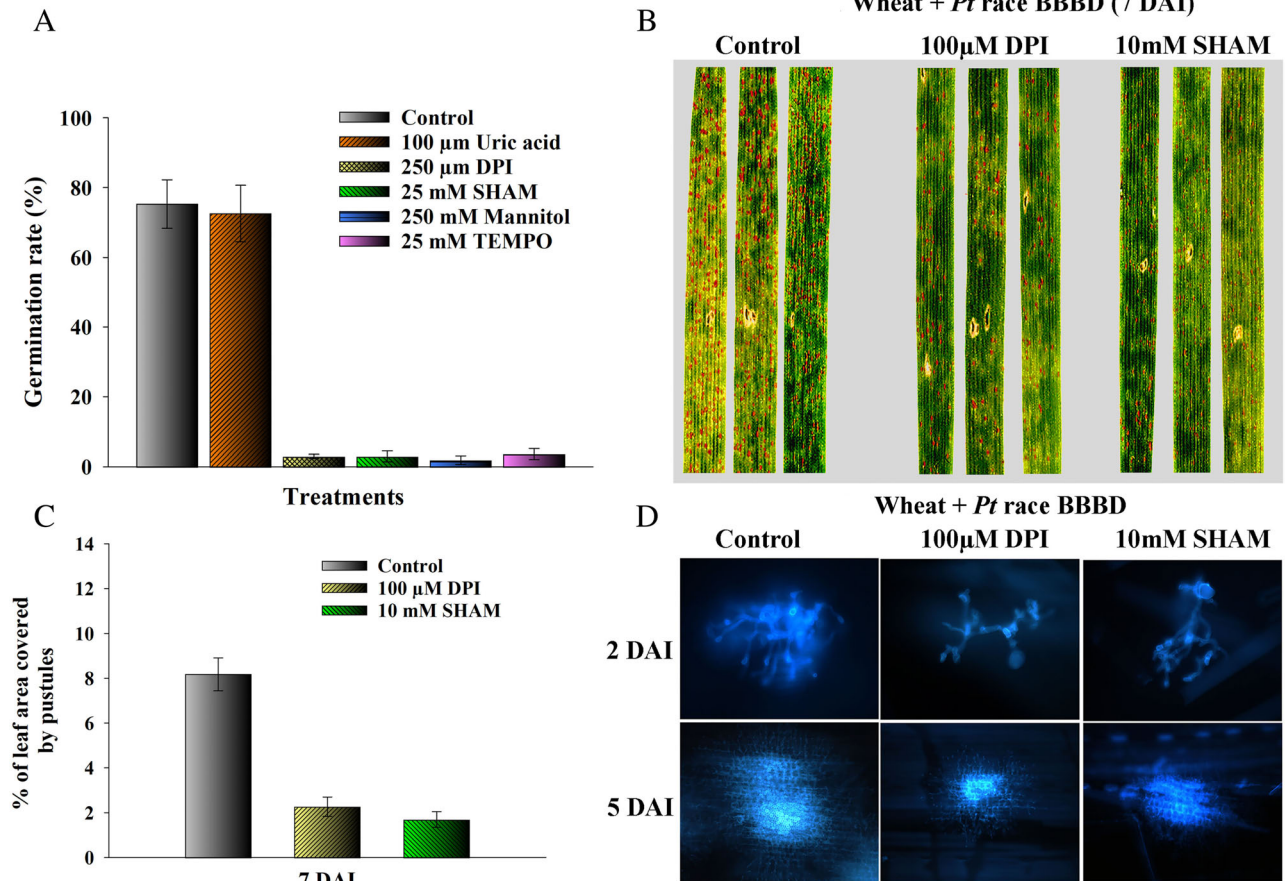


Fig 3. Effects of antioxidants and ROS scavengers on *Pt* urediniospore germination and virulence on wheat. A. Germination rates of *Pt* urediniospores on 2% agar containing antioxidants and ROS scavengers. B and C. Pustule formation of *Pt* on wheat leaves infiltrated with 100 μM DPI and 10 mM SHAM. D. Colony morphology of *Pt* in wheat leaves infiltrated with 100 μM DPI and 10 mM SHAM. Scale bars represent 10 μm . [Color figure can be viewed at wileyonlinelibrary.com]

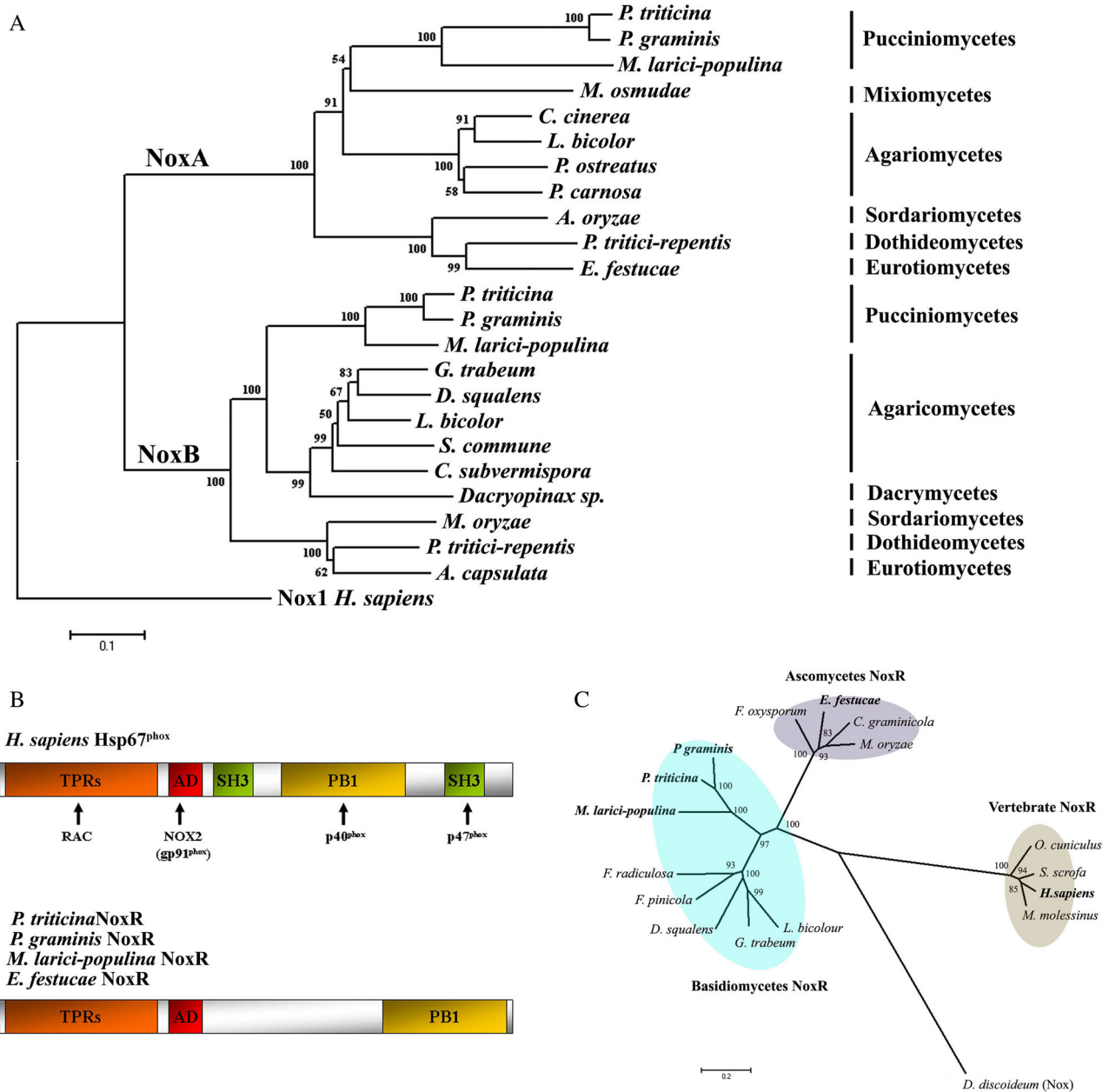


Fig 4. Molecular phylogeny of fungal NoxA, NoxB and NoxR proteins. **A.** Neighbour-joining phylogenetic tree of PtNoxA and PtNoxB with a selected group of fungal Nox proteins. The protein sequences were retrieved from UniprotKB database (<http://www.uniprot.org>) and aligned using the MAFFT program with default parameters. The phylogenetic tree was constructed using MEGA5 and rooted with *Homo sapiens* Nox1 (Q9Y5S8). Numbers at the nodes indicate the percentage of 1000 bootstrap replicates that support each labelled interior branch. **B.** Domain structures of *Pt*, *P. graminis*, *M. larici-populina* and *E. festucae* NoxR proteins compared to human p67^{phox} (Hsp67^{phox}). **C.** Phylogenetic relationships of *Pt* NoxR with other basidiomycete and ascomycete NoxR proteins and vertebrate p67^{phox}. The phylogenetic tree was constructed using MEGA5 using the neighbour-joining method and rooted with *Dictyostelium discoideum* (Do) Nox activator protein (Q867T7). Sequence data used in analysis can be found in the UniprotKB database under accession numbers; NoxA: *P. triticina* (A0A180G6Q1), *P. graminis* (E3JT61), *M. larici-populina* (F4RHR8), *M. osmundae* (G7DVS9), *C. cinerea* (A8N1A4), *L. bicolor* (B0CPG0), *P. ostreatus* (G5DE29), *P. carnosae* (K5WNU4), *A. oryzae* (I7ZXD1), *P. tritici-repentis* (B2W585), *E. festucae* (Q2PEP0); NoxB: *P. triticina* (A0A180H2F1); *P. graminis* (E3K1Z5), *M. larici-populina* (F4RMP4), *G. trabeum* (S7PW50), *D. squalens* (R7T012), *L. bicolor* (B0D4C9), *S. commune* (D8Q7W9), *C. subvermispora* (M2RDS7), *Dacryopinax sp.* (M5FS9), *M. oryzae* (L7JK22), *P. tritici-repentis* (B2W8H5), *A. capsulata* (C0NXS8); NoxR: *P. triticina* (PtNoxR, A0A180G901), *P. graminis* (PgtNoxR, E3K1Z5), *M. larici-populina* (F4RMP4), *Epichloe festucae* (EfNoxR, A0JC82), *Fibroporia radiculosa* (Fr, J4GSZ5), *Fomitopsis pinicola* (Fp, S8FAU2), *Dichomitrus squalens* (Ds, R7SHX9), *Gloeophyllum trabeum* (Gt, S7RQ35), *Laccaria bicolor* (Lb, B0D0Z3), *Fusarium oxysporum* (Fo, F9F3C0), *Collototrichum graminicola* (Cg, E3Q2G6), *Magnaporthe oryzae* (Mo, L7J9G7), *Oryctolagus cuniculus* (Oc, Q95MN2), *Sus scrofa* (Ss, B1PK10); *Musculus molesinus* (Mm, Q1PCS1). [Color figure can be viewed at wileyonlinelibrary.com]

and *PtSod* (PTTG_06754), encoding a putative catalase and a putative superoxide dismutase, were also identified.

A phylogenetic analysis comparing sequences of putative fungal NoxA and NoxB was performed. Among Basidiomycota, Nox orthologs were identified in species from Pucciniomycetes, Mixiomycetes and Agaricomycetes, but not from Ustilaginomycetes. The putative NoxA and NoxB from *Pt* and *Puccinia graminis* (*Pg*) are closely related (94% and 92% identity respectively) (Fig. 4a). A conserved N-terminal region containing four tetratricopeptide repeats and a putative activation domain were found in the predicted NoxR from *Pt*, *Pg*, *Melampsora larici-populina* and *Epichloë festucae*. At the C-terminus, all these fungal NoxR had a modified type of PB1 domain, which is required for the interaction of p67^{phox} with p47^{phox} and p40^{phox} in human (Fig. 4b). The phylogenetic analysis of NoxR from a selected group of fungi showed that the putative NoxR from *Pt*, *P. graminis* and *M. larici-populina* formed a subclade that was separated from other basidiomycetes and ascomycetes (Fig. 4c).

Variations in the transcript level of five *Pt* genes related to oxidation–reduction during *Pt* germination and in planta

The transcript levels of *PtNoxA*, *PtNoxB*, *PtNoxR*, *PtCat* and *PtSod* were quantified using RT-qPCR during the germination of *Pt* urediniospores over water (Fig. 5a) and in planta (Fig. 5b). During the germination of urediniospores, all five genes were up-regulated from 6 to 24 h after germination. There was a sharp increase in the transcript level of *PtNoxR* with a 9.3 ± 0.9 fold increase in its relative concentration at 24 h after germination. In *planta*, the expressions of *PtNoxA*, *PtNoxB*, *PtNoxR* and *PtCat* all appeared to be down-regulated from 12 to 120 HAI. In comparison, *PtSod* was up-regulated from 12 to 120 HAI during wheat infection. The highest concentration of *PtSod* was found at 120 HAI with a 9.8 ± 0.5 fold increases over the pre-inoculation level.

Discussion

ROS play a dual role in host–pathogen interactions. The endogenous ROS production of fungal pathogens is known to play important roles in regulating key developmental processes that are necessary for virulence (Morita *et al.*, 2013; Ryder *et al.*, 2013). However, the host oxidative burst is often induced as the first basal line of defence in a host upon recognition of a pathogen. As biotrophic fungal pathogens feed off living hosts, it is imperative for them to neutralize this response to evade the host immune system. It has been shown that full virulence of *U. maydis* depends on its ability to detoxify ROS during the infection process (Molina and Kahmann, 2007). In

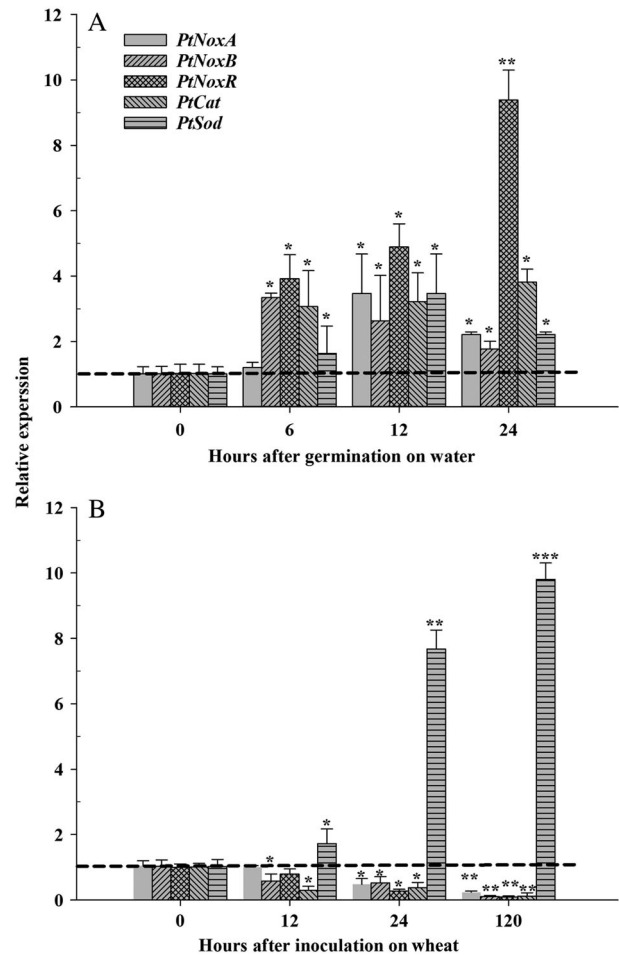


Fig 5. RT-qPCR analysis of *PtNoxA*, *PtNoxB*, *PtNoxR*, *PtCat* and *PtSod* transcripts during *Pt* urediniospore germination over water and its infection on wheat. A. *Pt* urediniospore germination over water. B. *Pt* infection on wheat. The constitutively expressed *Pt* succinate dehydrogenase gene was used for the normalization. Error bars depicted standard deviation from three independent biological repeats. Asterisk or double asterisk over bars within each gene represented statistical differences analysed using student *T*-test ($P \leq 0.01$).

AM fungi, an oxidative burst is thought to be beneficial for the establishment of a successful infection. (Kapoor and Singh, 2017).

In this study, we found that ROS are produced in various *Pt* structures that are critical for the successful infection of wheat. Among these structures, appressoria and substomatal vesicles are produced early during *Pt* penetration of the wheat surface, whereas intercellular infection hyphae and haustoria are produced later during the course of the infection process. The disruption of ROS production using a set of pharmacological inhibitors sharply decreased *Pt* urediniospore germination and intercellular growth. These results seem to be in the line with what has been reported for *Pst* where the treatment of *Pst* urediniospores with DPI reduced the germination

rate and germ tube length (Yin *et al.*, 2016). Based on this evidence, we conclude that ROS are critical for the full virulence of *Pt*.

ROS appear to be more concentrated in the actively growing regions of *Pt*. Localized production of ROS at growing hyphal tips has been reported in several fungal species, including *M. oryzae*, *E. festucae* and *A. alternata* (Tanaka *et al.*, 2006; Egan *et al.*, 2007; Morita *et al.*, 2013). In *M. oryzae*, the generation of ROS is crucial for hyphal tip growth and the differentiation of appressoria. The disruption of ROS production using inhibitor DPI results in a lower conidiospore germination rate and aberrant morphology of appressoria (Egan *et al.*, 2007). It has been shown that ROS regulate polarized fungal growth by remodelling the arrangement of the F-actin cytoskeleton, and the depolymerization of appressorial F-actin is competitively inhibited by ROS (Ryder *et al.*, 2013). In *A. alternata*, H₂O₂ is produced in appressoria during its infection on pear. A Δ *noxB* disruption mutant produced less ROS and was unable to penetrate the host cuticle, hence becoming non-pathogenic to the susceptible cultivar Nijisseiki (Morita *et al.*, 2013). These results together with our observations suggest that the production of ROS in *Pt* may contribute to defining a dominant polarity axis in actively growing regions of this fungus.

We deduced a likely generation of HO[·] in *Pt* infection structures. It has been reported that the production of HO[·], catalysed by cell wall-bound peroxidases, is essential for cleaving of cell wall polysaccharides and cell-wall loosening (Schweikert *et al.*, 2002; Liskay *et al.*, 2004). In the initial phase of infection, *Pt* goes through extensive growth and produces infection structures with different morphologies and functions, mainly fuelled by nutrient reserves stored in the urediniospore (Leonard and Szabo, 2005). It is likely that HO[·] may function as the cell wall loosening agent which is important for changes in cell wall chemistry during *Pt* infection to facilitate germ tube/hyphal extension and the differentiation of special infection structures.

During *Pt* penetration through the leaf surface, ROS are detected in wheat stomatal guard cells in contact with *Pt* appressoria. ROS are mainly distributed along the inner pore of guard cells. If these radicals associated with affected guard cells originate from *Pt*, it suggests that they diffuse across *Pt* cell membranes onto wheat guard cells during the penetration. An alternative possibility is that it is a response of wheat guard cells to *Pt* appressoria, possibly triggered by effectors that *Pt* secretes. It is known that ROS could induce stomatal closure, thus promoting plant immunity against pathogens entering through stomata. As the stomatal opening is the only point of entry for *Pt* during wheat infection, this response apparently should have a negative impact on *Pt* entry into the plant. However, this response does not inhibit the penetration of *Pt* through

wheat stomata because we observed the formation of *Pt* infection structures in the stomatal cavities underneath affected wheat guard cells in most infection sites. We can only speculate that this is due to the timing of stomatal closure induced by ROS. The stomatal closure occurs after *Pt* has penetrated the stomatal opening in a successful infection. Because high humidity is critical for *Pt* infection on wheat, the closure of stomata after *Pt* penetration through the leaf surface could provide an enclosed substomatal cavity with a micro-environment that is conducive for the survival of substomatal vesicles and primary infection hyphae. The other explanation is that *Pt* can just block stomatal closure downstream of ROS production during the penetration process.

The interaction between *Pt* and wheat during the stomatal penetration process is also quite interesting in the context of wheat resistance to rust fungi. In wheat, the defence response against rust pathogens is primarily post-haustorial. In this type of interaction, the haustorium-host cell interface plays an important role in host-pathogen recognition (Bolton *et al.*, 2008). However, several recent studies have indicated that pre-haustorial interaction also contributes to cereal rust resistance. Serfling *et al.* (2016) reported that the rust resistance in Einkorn (*Triticum monococcum*) is a pre-haustorial type of resistance that results in the non-formation of haustorial mother cells due to a rapid HR. In the interaction between wheat-*Lr9* and avirulent *Pt* race BBBB, the accumulation of callose is quickly induced in wheat guard cells in contact with *Pt* appressoria, which prevents the formation of infection hyphae and haustoria (Wang *et al.*, 2012). Similarly, the production of callose is induced within 24 h in wheat guard cells contacted by a *Pg* appressorium in incompatible interactions in wheat lines carrying *Sr36* or *Sr5*. In these interactions, *Pg* ingress is inhibited following the formation of the appressorium (Wang *et al.*, 2015). In the resistance response mediated by the stem rust R protein RPG1, two protein effectors associated with the stem rust urediniospore surface work cooperatively to activate RPG1 long before haustoria formation (Nirmala *et al.*, 2011). Based on this information, the interaction between *Pt* appressorium-wheat guard cell and its role in the initiation of the pre-haustorial resistance to rust fungi are quite interesting research areas that deserve more attention in the future.

We identified 291 unique *Pt* transcripts related to the function of oxidation and reduction in the *Pt* transcriptome produced during wheat infection. It is likely that *Pt* has a robust system to regulate endogenous ROS production and mediate redox homeostasis during wheat infection. In addition, a mechanism of neutralizing and suppressing the production of host ROS to escape the host immune responses may be also quite important for *Pt* because it is a biotrophic fungus feeding off living host cells without causing any symptoms.

Many multicellular organisms actively produce ROS via Nox complexes (Finkel, 2003; Heller and Tudzynski, 2011; Ryder *et al.*, 2013). In this study, both *Pt* urediniospore germination and subsequent intercellular growth were inhibited by DPI, a substrate inhibitor of Nox. We identified two putative Nox genes (*PtNoxA* and *PtNoxB*) in the *Pt* transcriptomes from different infection stages. The expression level of these Nox genes is lower *in planta* than in the pre-infection stage (during urediniospore germination). These results suggest that the generation of ROS in *Pt* is Nox-dependent. A coordinated down-regulation of these *PtNox* genes may be required to limit the hyphal growth rate during its biotrophic infection in plants or evade the host immune system.

Two paralogues of Nox (NoxA and NoxB) have been identified in fungal species including *E. festucae* (Tanaka *et al.*, 2006), *M. oryzae* (Ryder *et al.*, 2013) and *P. anserina* (Ryder *et al.*, 2013). The putative *PtNoxR* is structurally similar to *E. festucae* NoxR, a fungal homologue of the phagocytic p67^{phox} Nox regulator. NoxR has been shown to regulate both NoxA and NoxB. During the symbiosis of *E. festucae*, NoxR is a key regulator of NoxA which regulates the generation of ROS and controls hyphal growth by interacting with the small GTP binding protein RAC (Takemoto *et al.*, 2006). The exact functions of these *PtNox* genes in *Pt* virulence remain unclear. Host-induced gene silencing of these genes will be helpful in demonstrating the mechanism of Nox-dependent ROS production in *Pt*, and other potential roles of these *PtNox* genes.

Among ROS-scavenging enzymes, superoxide dismutase and catalase are the two most studied enzymes. Superoxide dismutase catalyses the dismutation of the superoxide radical to H₂O₂, which can then be further converted to H₂O by catalases. In *Pst*, it is found that *PsSOD1*, a zinc-only superoxide dismutase gene, is up-regulated within 24 h during wheat infection. The over-expression of *PsSOD1* in *Saccharomyces cerevisiae* confers enhanced stress tolerance to exogenous superoxide, whereas the knockdown of *PsSOD1* using a host-induced gene silencing method reduced the virulence of *Pst* on wheat. It is speculated that *PsSOD1* could contribute to *Pst* infection by scavenging host-derived ROS (Liu *et al.*, 2016). In this study, we observed a stronger expression of *PtSod* *in planta* compared to the germination stage (pre-infection). Because both *Pt* and *Pst* are obligate biotrophs that need to deal with host-derived ROS, we speculate that *PtSod* and *PstSOD1* have a role similar role in the virulence of these pathogens. *PtSod* may contribute to *Pt* virulence by scavenging host-derived ROS during wheat infection.

In summary, we demonstrate that ROS are critical for the full virulence of *Pt*. In future studies, higher priorities should be given to investigating the exact role of these putative *PtNox* genes in the pathogenesis of *Pt*, the

regulation of *Pt* genes related to ROS biosynthesis and the role of *Pt*-derived ROS in the interaction between *Pt* and wheat.

Acknowledgements

We would like to acknowledge the Ontario Ministry of Research and Innovation, Agriculture and Agri-Food Canada and Trent University for their financial support on this project. Authors declare no conflict of interest.

References

- Aguirre, J., Ríos-Momberg, M., Hewitt, D., and Hansberg, W. (2005) Reactive oxygen species and development in microbial eukaryotes. *Trends Microbiol* **13**: 111–118.
- Bashandy, T., Guilleminot, J., Vernoux, T., Caparros-Ruiz, D., Ljung, K., Meyer, Y., and Reichheld, J.-P. (2010) Interplay between the NADP-linked thioredoxin and glutathione systems in arabidopsis auxin signaling. *Plant Cell* **22**: 376–391.
- Bolton, M.D., Kolmer, J.A., and Garvin, D.F. (2008) Wheat leaf rust caused by *Puccinia triticina*. *Mol Plant Pathol* **9**: 563–575.
- Chernyak, B.V., Izyumov, D.S., Lyamzaev, K.G., Pashkovskaya, A.A., Pletjushkina, O.Y., Antonenko, Y.N., *et al.* (2006) Production of reactive oxygen species in mitochondria of HeLa cells under oxidative stress. *Biochim Biophys Acta* **1757**: 525–534.
- Cuomo, C.A., Bakkeren, G., Khalil, H.B., Panwar, V., Joly, D., Linning, R., *et al.* (2017) Comparative analysis highlights variable genome content of wheat rusts and divergence of the mating loci. *G3* **7**: 361–376.
- Dietz, K.-J., Mittler, R., and Noctor, G. (2016) Recent progress in understanding the role of reactive oxygen species in plant cell signaling. *Plant Physiol* **171**: 1535–1539.
- Dmochowska-Boguta, M., Nadolska-Orczyk, A., and Orczyk, W. (2013) Roles of peroxidases and NADPH oxidases in the oxidative response of wheat (*Triticum aestivum*) to brown rust (*Puccinia triticina*) infection. *Plant Pathol* **62**: 993–1002.
- Dobin, A., Davis, C.A., Schlesinger, F., Drenkow, J., Zaleski, C., Jha, S., *et al.* (2013) STAR: ultrafast universal RNA-seq aligner. *Bioinformatics* **29**: 15–21.
- Egan, M.J., Wang, Z.-Y., Jones, M.A., Smirnov, N., and Talbot, N.J. (2007) Generation of reactive oxygen species by fungal NADPH oxidases is required for rice blast disease. *Proc Natl Acad Sci U S A* **104**: 11772–11777.
- Finkel, T. (2003) Oxidant signals and oxidative stress. *Curr Opin Cell Biol* **15**: 247–254.
- Fofana, B., Banks, T.W., McCallum, B., Strelkov, S.E., and Cloutier, S. (2007) Temporal gene expression profiling of the wheat leaf rust pathosystem using cDNA microarray reveals differences in compatible and incompatible defence pathways. *Int J Plant Genom* **2007**: 17542. <https://doi.org/10.1155/2007/17542>.
- Foreman, J., Demidchik, V., Bothwell, J.H.F., Mylona, P., Miedema, H., Torres, M.A., *et al.* (2003) Reactive oxygen species produced by NADPH oxidase regulate plant cell growth. *Nature* **422**: 442–446.

- Freinbichler, W., Colivicchi, M., Stefanini, C., Bianchi, L., Ballini, C., Misini, B., et al. (2011) Highly reactive oxygen species: detection, formation, and possible functions. *Cell Mol Life Sci* **68**: 2067–2079.
- Giesbert, S., SchÜRg, T., Scheele, S., and Tudzynski, P. (2008) The NADPH oxidase Cpnox1 is required for full pathogenicity of the ergot fungus *Claviceps purpurea*. *Mol Plant Pathol* **9**: 317–327.
- Hagborg, W.A.F. (1970) A device for injecting solutions and suspensions into thin leaves of plants. *Can J Bot* **48**: 1135–1136.
- Heller, J., and Tudzynski, P. (2011) Reactive oxygen species in phytopathogenic fungi: signaling, development, and disease. *Annu Rev Phytopathol* **49**: 369–390.
- Hyon, G.-S., Ikeda, K.-i., Hosogi, N., Shinogi, T., and Park, P. (2010) Inhibitory effects of antioxidant reagent in reactive oxygen species generation and penetration of appressoria of *Alternaria alternata* Japanese pear pathotype. *Phytopathology* **100**: 840–847.
- Kapoor, R., and Singh, N. (2017) Arbuscular mycorrhiza and reactive oxygen species. In *Arbuscular mycorrhizas and stress tolerance of plants*: The Netherlands: Springer, pp 225–243.
- Katoh, K., and Standley, D.M. (2013) MAFFT multiple sequence alignment software version 7: improvements in performance and usability. *Mol Biol Evol* **30**: 772–780.
- Kwak, J.M., Mori, I.C., Pei, Z.M., Leonhardt, N., Torres, M. A., Dangl, J.L., et al. (2003) NADPH oxidase *AtrbohD* and *AtrbohF* genes function in ROS-dependent ABA signaling in *Arabidopsis*. *EMBO J* **22**: 2623–2633.
- Leonard, K.J., and Szabo, L.J. (2005) Stem rust of small grains and grasses caused by *Puccinia graminis*. *Mol Plant Pathol* **6**: 99–111.
- Liszskay, A., van der Zalm, E., and Schopfer, P. (2004) Production of reactive oxygen intermediates (O_2^- , H_2O_2 , and $\cdot OH$) by maize roots and their role in wall loosening and elongation growth. *Plant Physiol* **136**: 3114–3123.
- Liu, J., Guan, T., Zheng, P., Chen, L., Yang, Y., Huai, B., et al. (2016) An extracellular Zn-only superoxide dismutase from *Puccinia striiformis* confers enhanced resistance to host-derived oxidative stress. *Environ Microbiol* **18**: 4118–4135.
- Livak, K., and Schmittgen, T. (2001) Analysis of relative gene expression data using real-time quantitative PCR and the $2^{-\Delta\Delta CT}$ method. *Methods* **25**: 402–408.
- Marschall, R., and Tudzynski, P. (2016) Reactive oxygen species in development and infection processes. *Semin Cell Dev Biol* **57**: 138–146.
- McCallum, B.D., Seto-Goh, P., and Xue, A. (2013) Physiologic specialization of *Puccinia triticina*, the causal agent of wheat leaf rust, in Canada in 2009. *Can J Plant Pathol* **35**: 338–345.
- Michan, S., Lledias, F., Baldwin, J.D., Natvig, D.O., and Hansberg, W. (2002) Regulation and oxidation of two large monofunctional catalases. *Free Rad Biol Med* **33**: 521–532.
- Molina, L., and Kahmann, R. (2007) An *Ustilago maydis* gene involved in H_2O_2 detoxification is required for virulence. *Plant Cell* **19**: 2293–2309.
- Morita, Y., Hyon, G.-S., Hosogi, N., Miyata, N., Nakayashiki, H., Muranaka, Y., et al. (2013) Appressorium-localized NADPH oxidase B is essential for aggressiveness and pathogenicity in the host-specific, toxin-producing fungus *Alternaria alternata* Japanese pear pathotype. *Mol Plant Pathol* **14**: 365–378.
- Nirmala, J., Drader, T., Lawrence, P.K., Yin, C., Hulbert, S., Steber, C.M., et al. (2011) Concerted action of two avirulent spore effectors activates reaction to *Puccinia graminis* 1 (*Rpg1*) mediated cereal stem rust resistance. *Proc Natl Acad Sci U S A* **108**: 14676–14681.
- Panwar, V., McCallum, B., and Bakkeren, G. (2013) Endogenous silencing of *Puccinia triticina* pathogenicity genes through in planta-expressed sequences leads to the suppression of rust diseases on wheat. *Plant J* **73**: 521–532.
- Robinson, K.M., Janes, M.S., Pehar, M., Monette, J.S., Ross, M.F., Hagen, T.M., et al. (2006) Selective fluorescent imaging of superoxide *in vivo* using ethidium-based probes. *Proc Natl Acad Sci U S A* **103**: 15038–15043.
- Ryder, L.S., Dagdas, Y.F., Mentlak, T.A., Kershaw, M.J., Thornton, C.R., Schuster, M., et al. (2013) NADPH oxidases regulate septin-mediated cytoskeletal remodeling during plant infection by the rice blast fungus. *Proc Natl Acad Sci U S A* **110**: 3179–3184.
- Schweikert, C., Liszkay, A., and Schopfer, P. (2002) Polysaccharide degradation by Fenton reaction-or peroxidase-generated hydroxyl radicals in isolated plant cell walls. *Phytochemistry* **61**: 31–35.
- Serfling, A., Templer, S.E., Winter, P., and Ordon, F. (2016) Microscopic and molecular characterization of the prehaustorial resistance against wheat leaf rust (*Puccinia triticina*) in Einkorn (*Triticum monococcum*). *Front Plant Sci* **7**: 1668–1668.
- Setsukinai, K., Urano, Y., Kakinuma, K., Majima, H.J., and Nagano, T. (2003) Development of novel fluorescence probes that can reliably detect reactive oxygen species and distinguish specific species. *J Biol Chem* **278**: 3170–3175.
- Sewelam, N., Kazan, K., and Schenk, P.M. (2016) Global plant stress signaling: reactive oxygen species at the cross-road. *Front Plant Sci* **178**. <https://doi.org/10.3389/fpls.2016.00187>.
- Takemoto, D., Tanaka, A., and Scott, B. (2006) A p67Phox-like regulator is recruited to control hyphal branching in a fungal–grass mutualistic symbiosis. *Plant Cell* **18**: 2807–2821.
- Tamura, K., Peterson, D., Peterson, N., Stecher, G., Nei, M., and Kumar, S. (2011) MEGA5: molecular evolutionary genetics analysis using maximum likelihood, evolutionary distance, and maximum parsimony methods. *Mol Biol Evol* **28**: 2731–2739.
- Tanaka, A., Christensen, M.J., Takemoto, D., Park, P., and Scott, B. (2006) Reactive oxygen species play a role in regulating a fungus–perennial ryegrass mutualistic interaction. *Plant Cell* **18**: 1052–1066.
- Torres, M.A., Jones, J.D.G., and Dangl, J.L. (2006) Reactive oxygen species signaling in response to pathogens. *Plant Physiol* **141**: 373–378.
- Trapnell, C., Williams, B.A., Pertea, G., Mortazavi, A., Kwan, G., van Baren, M.J., et al. (2010) Transcript assembly and quantification by RNA-Seq reveals unannotated transcripts and isoform switching during cell differentiation. *Nat Biotechnol* **28**: 511–515.

- Venice, F., de Pinto, M.C., Novero, M., Ghignone, S., Salvioli, A., and Bonfante, P. (2017) *Gigaspora margarita* with and without its endobacterium shows adaptive responses to oxidative stress. *Mycorrhiza* **27**: 747–759.
- Wang, X., McCallum, B.D., Fetch, T., Bakkeren, G., Marais, G.F., and Saville, B.J. (2012) Comparative microscopic and molecular analysis of Thatcher near-isogenic lines with wheat leaf rust resistance genes *Lr2a*, *Lr3*, *LrB* or *Lr9* upon challenge with different *Puccinia triticina* races. *Plant Pathol* **62**: 698–707.
- Wang, X., McCallum, B.D., Fetch, T., Bakkeren, G., and Saville, B.J. (2015) *Sr36*- and *Sr5*-mediated resistance response to *Puccinia graminis* f. sp. *tritici* is associated with callose deposition in wheat guard cells. *Phytopathology* **105**: 728–737.
- Wojtaszek, P. (1997) Oxidative burst: an early plant response to pathogen infection. *Biochem J* **322**: 681–692.
- Yin, S., Gao, Z., Wang, C., Huang, L., Kang, Z., and Zhang, H. (2016) Nitric oxide and reactive oxygen species coordinately regulate the germination of *Puccinia striiformis* f. sp. *tritici* urediniospores. *Front Microbiol* **23**: 178. <https://doi.org/10.3389/fmicb.2016.00178>.
- Zhao, Y.L., Zhou, T.T., and Guo, H.S. (2016) Hyphopodium-specific VdNoxB/VdPls1-dependent ROS-Ca²⁺ signaling is required for plant infection by *Verticillium dahliae*.

PLoS Pathogens **12**. <https://doi.org/10.1371/journal.ppat.1005793>.

Supporting Information

Additional Supporting Information may be found in the online version of this article at the publisher's web-site:

Supplemental Table S1. The depth of libraries generated by RNA Illumina sequencing and alignment statistics to the *Pt* reference genome.

Supplemental Table S2. Real time quantitative PCR primers and conditions.

Supplemental Table S3. Gene ID, annotation and FPKM values of *Pt* transcripts that found to be associated with the function of general redox homeostasis.

Supplemental Figure S1. Gene ontology analysis of *Pt* genes identified in the RNA-Seq analysis. (a) Pie chart showing the distribution of *Pt* genes with specific GO terms; (b) heat map illustrating changes in expression levels of 37 *Pt* transcripts annotated with known functions in different stages of the infection process. Data represent normalized FPKM values and were Log₂-transformed; genes with similar patterns are clustered. The relative expression levels are colour-coded: red higher, and blue lower expression levels.